# An integrated topology optimization framework for 3D domains using shell elements

Giulia Angelucci [1]*, Seymour M. J. Spence [2], Fabrizio Mollaioli [1]

[1]Department of Structural Engineering and Geotechnics (DISG), Sapienza University of Rome
[2] Department of Civil and Environmental Engineering, University of Michigan

***Correspondence**:
Giulia Angelucci, Department of Structural Engineering and Geotechnics (DISG), Sapienza University of Rome, Via Gramsci 53, 00197, Rome, Italy. Tel.: (+39) 06-49919-186. Fax: (+39) 06-322-1449.
Email: giulia.angeluccini roma1.it

**ABSTRACT**

In the last decades, topology optimization has been widely investigated as a preliminary design tool to minimize the use of material in a structure. Despite this, applications to realistic three-dimensional engineering problems are still limited. This study provides the instruments for the definition of a versatile and integrated framework in order to apply topology optimization to large-scale 3D domains for the design of efficient and high-performing structures. The paper proposes a novel topology optimization strategy to identify the optimal layout of lateral resisting systems for tall buildings through the adoption of Mindlin-Reissner shell elements for the discretization of the continuum design domain. The framework is based on the practical interoperability between Matlab, Ansys and CAD environments to incorporate optimization routines in the conceptual design phase of structural systems. Finally, the paper examines a three-dimensional tall building case-study in order to demonstrate the applicability of the proposed procedure to realistic Civil Engineering design problems and its robustness in finding optimal layouts free from mesh-dependency instabilities.

KEYWORDS: Tall buildings, topology optimization, shell elements, mesh refinement, 3D optimization, integrated framework

## 1 Introduction

Topology optimization is widely recognized as a powerful preliminary design tool to determine the optimal material layout in a structure, i.e. the most effective configuration that reduces the consumption of structural material. The ability of finding innovative, efficient designs together with the improvement of computational tools has allowed, in the last decades, the possibility to carry out topology optimization with affordable computational cost. Most methods for topology optimization of continuum structures are based on the homogenization method and the SIMP (Solid Isotropic Material with Penalization) approach. In the homogenization method [1], a periodically micro-perforated structure is suggested and its micro-scale mechanical properties are expressed via the homogenization theory. The drawbacks associated with the evaluation of the optimal microstructure and the manufacturability of the resulting layout, led to the introduction of the SIMP method [2]. This methodology assumes a constant density distribution over the design domain where the stiffness matrix and the element density are interpolated through a heuristic power-law.

Since the release of the commercial software *Optishape* by Quint software in 1989, many other platforms have been developed to include topology optimization in the structural design process. Among them there are *Optistruct* (by Altair Computing), *Construct* (by MSC software), *Catopo* (by CES Eckard GmbH) and *TOSCA* (by FE-Design). Many optimization approaches and codes have also been interfaced with commercial FE solvers. For example, Altair *OptiStruct* uses Altair HyperWorks FE package while Ansys and *TOSCA* use the Ansys FE package. As many commercial design software companies have

equipped their products with structural optimization techniques in recent years, computer aided topology optimization has attracted increasing interest in the engineering community. Optimization tools developed by academics include the topology optimization program by Liu et al. [3] for Femlab, *ToPy* for Python [4], the 99-line program for Mathematica [5], the 99-line code [6] and the 88-line code [7] for Matlab. Based on the level-set method, Wang et al. [8] introduced *TOPLSM* for Matlab and Challis [9] developed the 129-line program. In 2013, Aage et al. [10] introduced *TopOpt*, the first topology optimization App. More recently, researchers have dedicated great effort towards the reduction of numerical anomalies related to the implementation of standard four-node quadrilateral elements (Q4) in topology optimization problems through proposing the use of alternative higher-order finite elements [11]–[14]. The use of unstructured finite element meshes was also extended to 3D domains with the introduction of *PolyTop3D* [15] and *Toptimiz3D* [16]. The main difficulties in dealing with large-scale applications are related to the following two aspects of the problem: handling of large data sets, and careful selection of proper finite elements (FE) for the discretization of the domain. Both aspects affect memory storage and processing requirements. Due to the abovementioned challenges, only a limited number of works have focused on topology optimization of 3D domains, with particular concentration on the use of eight-node hexahedral (brick) elements [17]–[20]. Although relevant results have been achieved, the use of solid elements leads to several drawbacks in the context of large-scale designs. First of all, a sufficient number of elements is needed to correctly model the thickness of the members in order to accurately capture the effects of bending stiffness. Furthermore, refining a solid mesh to improve the accuracy of the solution generally implies a huge number of elements, resulting in an increased number of slower iterations for achieving convergence. To overcome these challenges, this work is focused on the possibility of implementing shell elements for the discretization of 3D domains during the definition of optimal lateral loading resisting systems of multi-story steel buildings subject to winds loads through topology optimization. In the field of structural engineering, optimization techniques have been recently adopted to improve the overall response of tall buildings subject to critical excitations, e.g. the design of tuned mass dampers [21]–[26] or the best location for outrigger systems [27]–[30]. A considerable effort has also been made by researchers to perform the topology optimization of tall building systems subject to stochastic excitation, i.e. wind loads, seismic loads or integrated hazards [31]–[34].

It is generally assumed that a tall building, under wind loads, can be schematized as a cantilever beam with two flange faces resisting bending action and two web faces resisting shear forces. However, given the aleatory nature of the wind direction, each face will in general act simultaneously as a web and a flange, withstanding both in-plane and out-of-plane loads [35]. Because in shell elements, the membrane behavior is preserved and enriched with that of the plates, which carry transverse loads by bending and shear through out-of-plane stiffness, they appear especially suitable for the discretization of the design domain of three-dimensional tall buildings. Furthermore, the adoption of shells requires a reduced number of elements compared to solids, as they do not involve the modeling of the thickness, whose mechanical behavior is already included in the mathematical model. This significantly reduces the number of equations to be solved during the FE analysis and makes the use of shell elements more convenient than solid elements when iterative algorithms are inevitably implemented during the solution process. Finally, since shells can model curved and free-form designs and are compliant for software implementation, they are especially suitable for the discretization of complex 3D geometries and represent a valid option to perform topology optimization for modern designs. In the state-of-the-art, the problem of finding optimal topologies using shell elements is usually applied to problems focused on the definition of the optimal location of reinforcement in plate structures. Since plates suffer from poor overall rigidity, topology optimization represents an effective means to define the optimal layout of stiffeners [36]–[39]. Analogously to Q4 elements, shell elements may suffer from numerical instabilities and their implementation in density-based optimization procedures may produce mesh distortion, which may cause overestimation of the stiffness matrix and a checkerboarding pattern may occur. Bletzinger [40] and

Hassani et al. [41] implemented noise cleaning techniques to lessen the problem of mesh dependency in the resulting layouts. Boroomand and Barekatein [42] employed a sequential refinement strategy for the density-mesh together with a continuous field of density to alleviate instability effects. Pham and Phan have recently introduced polygonal plate elements (PRMn) to prevent the formation of checkerboarding patterns in the optimization of shell and plate structures [43].

The optimization problem dealt with here aims to find a maximum stiffness structural design for 3D tall buildings where the compliance of the structure is taken as the objective function and a constraint on the maximum available material is considered. The continuous domain, subject to out-of-plane and in-plane loadings, is modeled using Mindlin-Reissner (MR) shell elements. The SIMP model is adopted in formulating the topology optimization problem and a density filter is employed on the interpolation of the element elastic properties [44]. Mesh independent solutions are monitored by operating a gradual refinement of the mesh structure of the design domain. The paper presents the numerical results achieved by performing topology optimization on 3D case studies and highlights the advantages in the use of shell elements to discretize this class of domains. The work provides the instruments to overcome the limitations associated with large-scale domains and demonstrates the potential of topology optimization for 3D structures. This intent is made feasible by defining an integrated framework, which combines the efficiency of a reliable optimization algorithm, written in Matlab, with the advanced capabilities of Ansys (ANSYS® Academic Research Mechanical) for performing the finite element analysis.

## 2 Shell elements for continuum domains

The computational procedure for solving topology optimization problems must first deal with a spatial discretization of the continuum design domain. Most of the current topology optimization techniques have been applied to small-scale designs and implemented using four-node quadrilateral (Q4) elements, for two-dimensional domains, or eight-node brick (B8) elements, for three-dimensional domains. Many works have also emphasized investigating higher-order finite elements for 2D and 3D domains, which are naturally less susceptible to numerical instabilities. Although the topic of domain discretization using uniform or irregular meshes has been exhaustively investigated in the literature, shortcomings on the adequate finite element to be adopted are still present. The most commonly used elements for two-dimensional models are based on the traditional membrane formulation, with only two translational degrees of freedom (DOFs) per node ($u$ in x-direction and $v$ in y-direction). The membranes exhibit no flexural rigidity and, therefore, cannot withstand any out-of-plane load. In fact, they only transfer in-plane forces as a result of tensile and compressive stresses. Due to this, although membrane plane-stress elements have led to satisfactory results for two-dimensional problems, their implementation to three-dimensional cases may not provide equally accurate results in reproducing the real behavior of 3D structures. Three-dimensional domains, on the other hand, are generally analyzed using solid elements with three translational degrees of freedom per node ($u$ in x-direction, $v$ in y-direction and $w$ in z-direction). The main disadvantage in adopting bricks is that a large number of elements is required to correctly model the thickness of the domain and capture the effects of bending and stiffness. Furthermore, refining a solid mesh to improve the accuracy of the final solution involves a huge number of elements, which adds higher computational cost and further memory requirements. The aforementioned drawbacks associated with the tessellation of 3D domains using membrane or solid elements have naturally led this study towards the selection of alternative elements. In the specific case, the main assumption of the study is that the outer skin of the tall building is treated as a natural design domain, as depicted in **Figure 1**. The façades can be easily conceived as giant panels of small thickness, connected to each other along the panel joints and to the floor slabs at each floor level. Since one dimension of the design domain is much smaller than the other two, shell elements are particularly suitable for its discretization. Following this approach, the building skin is converted into equivalent shells, so that each panel can be assumed as a continuous design domain in which to apply topology optimization.

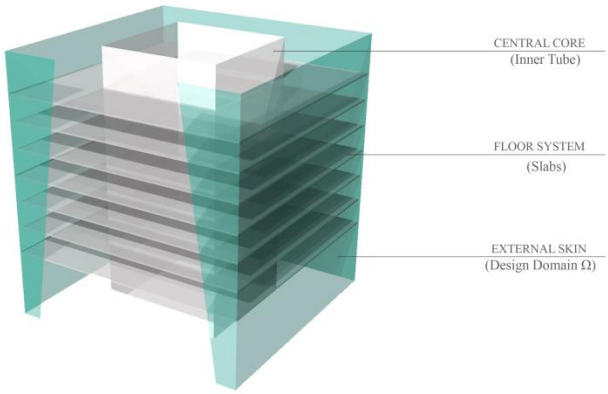


**Figure 1.** Schematic of the constitutive elements of a tall building.

Unlike membrane elements (**Figure 2 (a)**), shells can endure loads acting on the mid-surface of the element as well as transverse loads (**Figure 2 (b)**). Hence, in shell elements, the in-plane stiffness of the membrane is preserved and enriched with the out-of-plane stiffness of plates, which resist the transverse loads through bending and shear actions. In addition, the adoption of shells requires fewer elements to tessellate the thickness of the domain compared to solid bricks (**Figure 2 (c)**). This is mainly due to the fact that the mechanical behavior of the thickness is naturally included in the mathematical model of the shells. Moreover, only the stresses at the integration points are available for solid elements, while shell elements have the ability to account for the bending stress gradient across the thickness. This significantly reduces the number of equations to be solved during the FE-analysis and makes the use of shells more convenient than solids when iterative algorithms are executed. Furthermore, since shells can model curved and free-form designs and, they are especially suitable for the discretization of complex 3D tall buildings and represent a valid option for topology optimization routines.

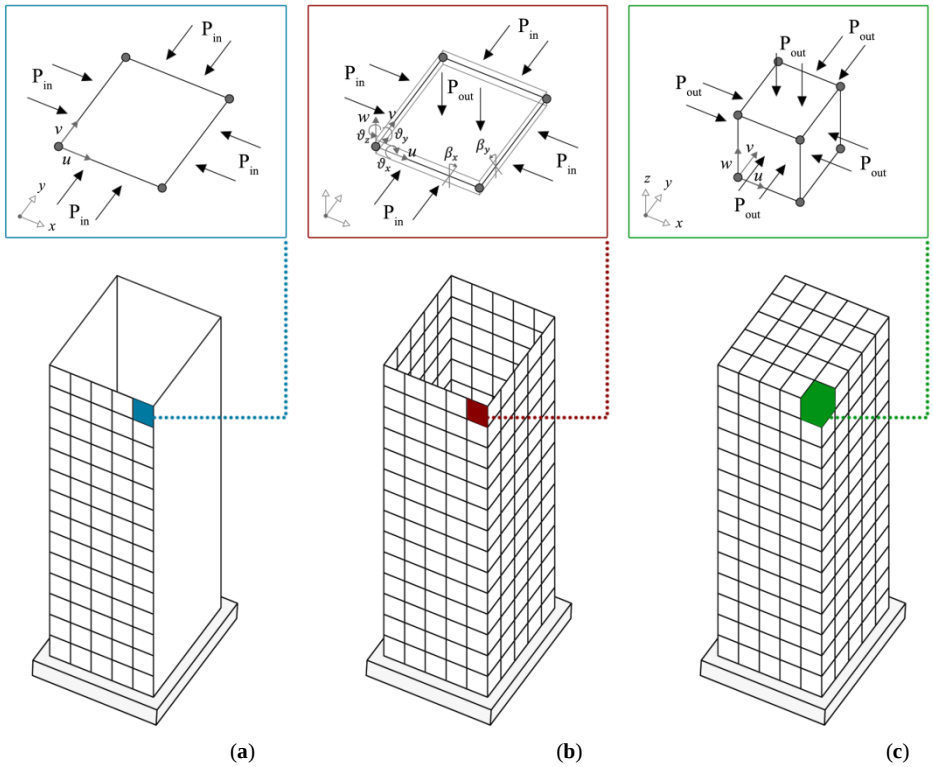


**Figure 2.** Domain discretization of a tall building using membrane elements **(a)**, shell elements **(b)** and solid elements **(c)**.

### 2.1 Element description and formulation

As already discussed, in the state of the art, finding optimal topologies using shell elements is generally posed as a problem of defining the optimal position of reinforcements in plate structures. Nevertheless, the potential advantages associated with the adoption of shell elements in topology optimization routines are far from being exhaustively investigated. To this end, a complete description of the finite element adopted, carefully chosen from those available in the Ansys database, is presented hereafter.

A 4-node shell element based on the Mindlin-Reissner plate theory (SHELL181) is chosen from the software library to discretize the design domain [45]. The element, illustrated in **Figure 2 (b)**, is defined by four nodes and has six DOFs per node, three translations (*u*, *v*, *w*) and three rotations (*Θx, Θy, Θz*). In addition to the five traditional DOFs, in fact, the element adopts a supplemental rotation about the normal to the plane of the element, the so-called "drilling" degree of freedom. Although this rotation is not explicitly required for the kinematics of the shell, it allows for a correct modeling of the connection with other shells or beam elements and helps to improve the accuracy of the numerical results. The shell is formulated as the combination of a membrane element, with in-plane behavior, and a plate element, with out-of-plane behavior. For the plate component, the first-order shear deformation theory of Mindlin-Reissner (MR) is employed. Assuming a plate with homogeneous and isotropic material and small displacements and strains with respect to its thickness, the pure bending component and the transverse shear contribution can be treated separately. This greatly simplifies the element formulation and helps preventing locking phenomena. According to this assumption, the element constitutive matrix for the MR plate can be formally written as the sum of the bending ($\mathbf{C}_b$) and the shear ($\mathbf{C}_s$) components. The flexural rigidity of the pure bending counterpart is given by:

$$\mathbf{C}_b = \frac{E_0 h^3}{12(1-\nu^2)} \begin{pmatrix} 1 & \nu & 0 \\ \nu & 1 & 0 \\ 0 & 0 & \frac{1-\nu}{2} \end{pmatrix} \tag{1}$$

where $\nu$ and $E_0$ are the Poisson's ratio and the elastic modulus of the structural material, respectively; $h$ is the shell thickness, which is assumed to be constant over the element. On the other hand, the contribution of the shear rigidity is given by:

$$\mathbf{C}_s = \frac{E_0 h \mu}{2(1+\nu)} \begin{pmatrix} 1 & 0 \\ 0 & 1 \end{pmatrix} \tag{2}$$

where $\mu$ is the shear correction factor, set to 5/6 [46].

After evaluating the section curvatures and the shear strains, the relative strain-displacement matrices ($\mathbf{B}_b$ and $\mathbf{B}_s$) and the element stiffness matrices of the plate component are directly constructed. The global stiffness matrix $\mathbf{K}_p$ of the MR plate element is formulated by integrating the separated contributions of the pure bending ($\mathbf{K}_b$) and the transverse shear ($\mathbf{K}_s$) over the area $A$ of the element, as follows:

$$\mathbf{K}_p = \mathbf{K}_b + \mathbf{K}_s = \int_A \mathbf{B}_b^T \mathbf{C}_b \mathbf{B}_b \, dA + \int_A \mathbf{B}_s^T \mathbf{C}_s \mathbf{B}_s \, dA \tag{3}$$

Finally, through assembly of the plate contribution $\mathbf{K}_p$ with the membrane counterpart $\mathbf{K}_m$, the stiffness matrix of the shell element (**K**) can be written as follows:

$$\mathbf{K} = \begin{pmatrix} \mathbf{K}_m & 0 \\ symm & \mathbf{K}_p \end{pmatrix} \tag{4}$$

where $\mathbf{K}_{\mathrm{m}} = \int_A \mathbf{B}_{\mathrm{m}}^{\mathrm{T}} \mathbf{C}_{\mathrm{m}} \mathbf{B}_{\mathrm{m}} \, \mathrm{d}A$ is the in-plane stiffness component of the shell, $\mathbf{B}_{\mathrm{m}}$ is the associated strain-displacement matrix and $\mathbf{C}_{\mathrm{m}}$ is the membrane constitutive matrix, defined as follows:

$$\mathbf{C}_{\mathrm{m}} = \frac{\mathrm{E}_0 h}{(1+\nu^2)} \begin{pmatrix} 1 & \nu & 0 \\ \nu & 1 & 0 \\ 0 & 0 & \dfrac{1-\nu}{2} \end{pmatrix} \tag{5}$$

It should be emphasized here that, in order to avoid undesirable shear-locking phenomena, the formulation of the 4-node MR plate element is modified by including the assumed strain interpolation of Bathe-Dvorkin [47]. It is a Mixed Interpolated Tensorial Component (MITC) method that constructs the stiffness matrix by including the bending and shear effects through different interpolations, producing many benefits. First, even when the element is highly distorted, a 2x2 standard Gauss integration is adequate and, since a full numerical integration is used, the element does not contain any spurious zero energy mode. Second, the element passes the patch test and does not lock even in the analysis of thin shells, i.e. its behavior is independent of the specific plate theory assumed. Hence, it can be concluded that the SHELL181 element is highly accurate, even with coarse meshes, and has a good predictive capability for displacements, bending moments and membrane forces. This is particularly favorable in the present case, since if shear-locking occurs, the stiffness of the structure might be significantly over-predicted with consequent underestimation of the displacements. A similar condition should always be avoided in topology optimization problems because it may negatively affect the results and undermine the objectivity of the final layouts, leading to undesirable effects such as checkerboarding.

### 2.2 Interpolated elastic properties

In order to find efficient solutions for the topology optimization problem, the Solid Isotropic Material with Penalization (SIMP) approach is adopted in this work with the modified scheme proposed by Sigmund in [48]. The mechanical properties of each shell element are manipulated using a heuristic power-law that relates the element-wise design variable ($x_e$) with the element elastic properties, through:

$$E_e(x_e) = E_{\min} + x_e^p (E_0 - E_{\min}), \quad 0 \le x_e \le 1 \tag{6}$$

where $e$=1,…,$n$ and $n$ is the total number of elements discretizing the domain, $E_{\min}$ is a small positive elastic modulus greater than zero to avoid any singularity of the global stiffness matrix, $E_0$ is the elastic modulus of the solid material. A penalty factor $p$ greater than zero, typically 3 or 5, is introduced to penalize the presence of intermediate densities in the relaxed setting and to steer the solution to binary 0-1 values.

Topology optimization using shell elements is performed based on the assumption that the stiffness matrix of each finite element is proportional to its "artificial" elastic modulus ($E_e$). By isolating the elastic modulus $E_0$ in Eqs. (1), (2) and (5), the constitutive matrices of element $e$ can be rewritten in a generalized form, as follows:

$$\mathbf{C}_e(x_e) = E_e(x_e)\mathbf{C}_e^0 \tag{7}$$

where $E_e$ is calculated using Eq. (6) and $\mathbf{C}_e{}^0$ is the generalized constitutive matrix with unit Young's modulus ($\mathbf{C}_{\mathrm{b}}{}^0$, $\mathbf{C}_{\mathrm{s}}{}^0$ and $\mathbf{C}_{\mathrm{m}}{}^0$). In the above equation $E_e$ is the only variable term, while the constitutive matrix is assumed to be constant. Using the finite element method, the stiffness matrix $\mathbf{K}_e$ of element $e$ is evaluated as the integral over the area of the element constitutive matrix $\mathbf{C}_e{}^0$ and the element strain-displacement matrix $\mathbf{B}_e$. Therefore, according to the SIMP approach, even the element stiffness matrix of Eq. (4) can be interpolated as follows:

$$\mathbf{K}_e(x_e) = E_e(x_e)\mathbf{K}_e^0 \tag{8}$$

where $\mathbf{K}_e^0$ is the element stiffness matrix of the material with unit Young's modulus. The global stiffness matrix is, therefore, obtained by assembling the element-level counterparts through:

$$\mathbf{K}(x_e) = \sum_{e=1}^{n} \mathbf{K}_e(x_e) = \sum_{e=1}^{n} E_e(x_e)\mathbf{K}_e^0 \tag{9}$$

Introducing the modified interpolation function in Eq. (6), the previous relation assumes the following form:

$$\mathbf{K}(x_e) = \sum_{e=1}^{n} (\mathrm{E}_{\min} + x_e{}^p(\mathrm{E}_0 - \mathrm{E}_{\min}))\mathbf{K}_e{}^0 \tag{10}$$

Finally, the nodal displacement vector $\mathbf{u}(x_e)$ is calculated as the solution of the equilibrium equation:

$$\sum_{e=1}^{n} (\mathrm{E}_{\min} + x_e^p(\mathrm{E}_0 - \mathrm{E}_{\min}))\mathbf{K}_e^0)\mathbf{u}(x_e) = \mathbf{F} \tag{11}$$

where $\mathbf{F}$ is the load vector independent of the design variables. It is significant to recall here that, in the relation above, $\mathbf{K}_e^0$ is a constant matrix and it is decoupled from the element fictitious densities, which are updated at each iteration. This is a crucial advantage for the construction of the topology optimization framework, since it allows to acquire the element stiffness data only once at the beginning of the procedure, speeding up the overall optimization process.

## 3 Problem statement

A standard "academic" formulation for topology optimization problems, commonly referred to as the design for minimum compliance or for maximum global stiffness, consists in minimizing the external work done by the applied loads (i.e. the mean compliance) subjected to a volume constraint. The mean compliance is a self-adjoint function, which makes the formulation straightforward when calculating the sensitivities, and allows for achieving good results at reduced computational cost. Due to these properties it is a widely used approach and is adopted herein. Discretizing the design domain using finite elements and using the same mesh for both the displacement (**u**) and the stiffness (**K**) fields, the topology optimization problem can be formally written in the following discrete relaxed form:

$$\begin{cases} \min\limits_{\boldsymbol{\rho}} \; c(\boldsymbol{\rho}) = \mathbf{F}^{\mathrm{T}}\mathbf{u}(\boldsymbol{\rho}) \\ \text{s.t.} \;\; V(\boldsymbol{\rho}) \le V_o \, volfrac \\ \qquad \mathbf{K}(\boldsymbol{\rho})\,\mathbf{u}(\boldsymbol{\rho}) = \mathbf{F} \\ \qquad 0 \le \rho_e \le 1, \quad e = 1,\ldots,n \end{cases} \tag{12}$$

where $c(\boldsymbol{\rho})$ is the mean compliance, which is a global measure of the stiffness of the structure; $\boldsymbol{\rho}(\mathbf{x})=\{\rho_1,\ldots,\rho_n\}^{\mathrm{T}}$ is the element-wise material density vector related to the independent design variable vector $\boldsymbol{x}$ through $\rho_1=\varphi_e(x_e)$; $x_e$ is the design variable assumed constant within each element; $\varphi_e$ is the filter operator (e.g. the H-filter [44]); $n$ is the total number of finite elements set equal to the number of design variables; *volfrac* is the volume fraction computed as the ratio between the actual volume of structural material in the design domain $V(\boldsymbol{\rho})$ and the initial volume $V_0$. Assuming an isotropic and homogeneous material, the volume of the structure can be evaluated as the integral of the design variables over the domain $\Omega$; therefore, $\boldsymbol{\rho}(\mathbf{x})$ can be referred to as a material density. In the following sections, we omit the dependence of the filtered densities $\boldsymbol{\rho}$ on the design variables $\mathbf{x}$, i.e. $\boldsymbol{\rho}=\boldsymbol{\rho}(\mathbf{x})$.

## 4 Implementation strategy

In this work, the topology optimization problem is performed by introducing a versatile framework based on the practical interoperability between Matlab, Ansys and CAD environments in order to create a robust procedure for practical engineering problems.

Ansys is a general-purpose commercial software package, which generates simulated computer models of structures, electronic elements or machines. The program package can perform structural, thermal, dynamic and fluid dynamic analyses. These capabilities may be integrated with the proposed framework and could encourage users to adopt it also in research fields other than Civil Engineering, opening new frontiers for topology optimization. The interactive use of Ansys Mechanical offers many benefits to the optimization procedure. First, by exploiting the interaction with neutral formats, such as IGES files, Ansys provides the possibility of importing CAD (Computer Aided Design) geometries into the mechanical data. Thus, a complete model can be generated with 3D modeling software and subsequently exported to the Ansys environment. This allows the framework to handle complex or articulated 2D and 3D geometries. Second, the use of external software allows the selection of appropriate finite element types from those available in the program library, e.g. membrane elements, shell elements or solid elements. Finally, different methods for solving the system of simultaneous equilibrium equations can be selected by the user in the Ansys database. In topology optimization problems, in fact, the finite element analysis is a computationally intensive part, in which up to 60% of numerical calculations are spent for the solution of a sequence of equilibrium equations in the form: $\mathbf{K}(\mathbf{x})\,\mathbf{u} = \mathbf{f}$ (where $\mathbf{K}$ is the stiffness matrix of the structure as a function of the design variables $\mathbf{x}$, $\mathbf{u}$ is the displacement vector and $\mathbf{f}$ is the load vector). In this study, the sparse direct method is adopted to solve the systems of linear equations. Since the factorization of the $\mathbf{K}$ is generally the most time-consuming phase in a serial implementation, the solver is based on a direct elimination of equations, which minimizes the cost of the factorizing using equation reordering strategies. This significantly reduces both the storage space needed and the work performed.

The methodology is conceived in a generalized form to handle a wide set of design problems. The flowchart of the proposed integrated framework for solving 2D and 3D large-scale topology optimization problems is illustrated in **Figure 3** and the main steps are discussed in the following sections and briefly introduced here.

*(i)* First, the geometrical and mechanical models are generated and the information required to perform the topology optimization procedure are stored.

*(ii)* The integrated framework is initialized to solve the minimum compliance problem stated in Eq. (12). The main loop of the framework starts with the finite element sub-routine, through a batch-mode call to Ansys Mechanical. In this stage, the finite element analysis is performed and the resulting nodal displacements are stored.

*(iii)* Next, a loop over the elements computes the objective and constraint functions with related sensitivity analyses. In order to update the design variables through the mathematical programming optimizer, the calculated sensitivities are converted to non-filtered quantities. The current structural compliance, the related volume constraint and the iteration number are printed and the resulting optimal material distribution is displayed. The convergence of the sub-problem in terms of the design variable vector is checked at each iteration.

Because the finite element analysis and the optimization routines are separately defined, the framework can be extended and easily modified in all its parts. In fact, the design domain, the loading and supporting conditions, the problem formulation and the optimization algorithm can be altered for adapting the procedure to different design needs. This work should be considered as the setting up of a robust generalized methodology, so that it can be adopted as a preliminary design tool for simplified loading conditions or interpreted as a sub-problem by including more complicated scenarios (e.g. stochastic loading conditions). In both cases, the procedure allows achieving reliable optimal layouts where the

precision of the resulting topologies depends on the accuracy of modeling and loading assumptions. The framework is adaptable and ready for integration since extensions and changes are ensured.

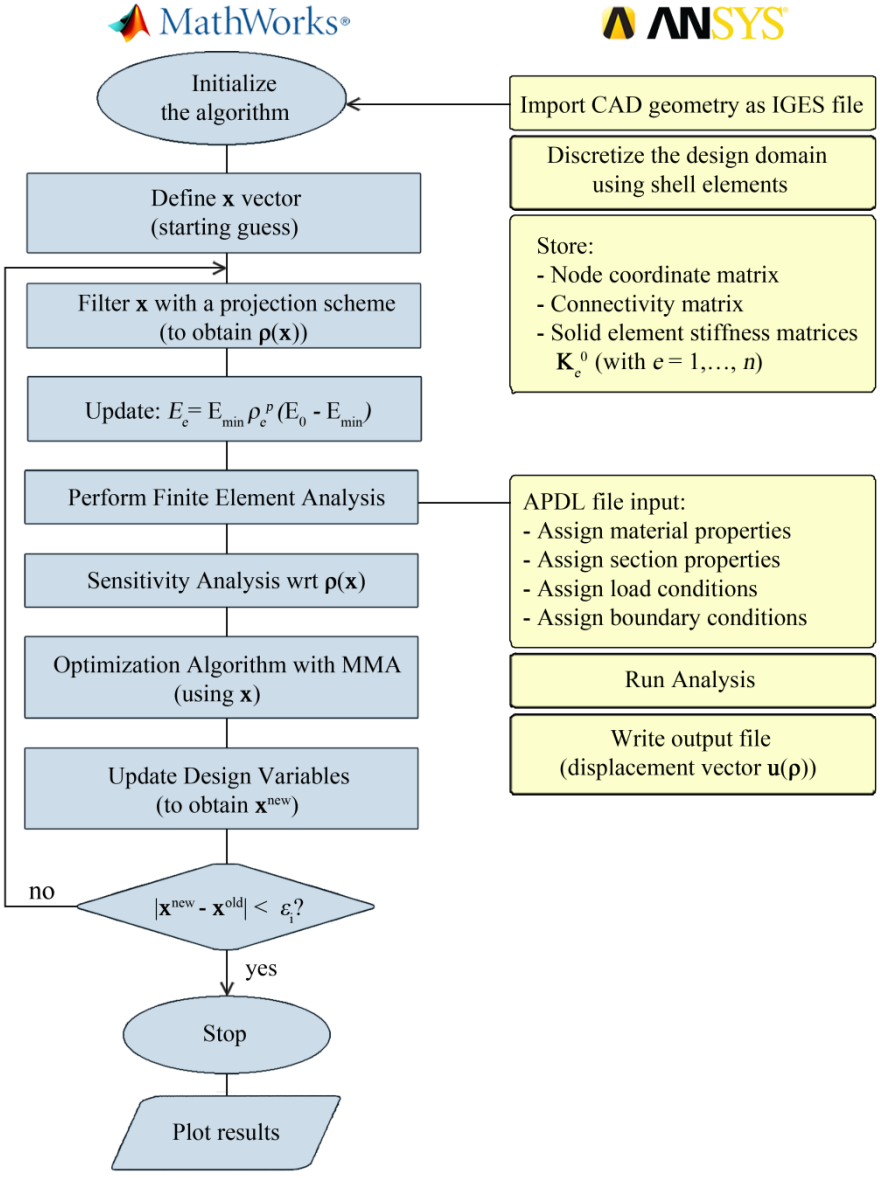


**Figure 3.** Flowchart of the proposed integrated framework.

### 4.1 Description of the integrated framework

As previously observed, Ansys Mechanical interacts with neutral formats, e.g. IGES files, allowing the possibility of importing regular or complex-shaped CAD geometries. The interaction with 3D modeling software strongly supports users in carefully drawing and managing the overall design. The first step of the proposed procedure concerns the design of the structural components within a general CAD environment, where a relevant preliminary phase consists in choosing a suitable continuum domain by selecting the parts of the model that should be designed and the parts that should be left as solids or voids in the final topology. At the beginning of the procedure, an Ansys APDL (Ansys Parametric Design Language) script is written, which contains the following operational commands: (*i*) import CAD geometries into the finite element software through an IGES file; (*ii*) assign material properties and

discretize the continuum domain using shell elements and (*iii*) store information on the geometrical and mechanical model.

For step (*i*), the script constructs the geometrical entities of the model (e.g. key-points, lines and area elements), based on the information acquired from the IGES file. In step (*ii*), element types are assigned to the corresponding elements, with sections of the structural members (e.g. cross-section of beam elements and thickness of shells) sized according to a preliminary design. The continuum domain is discretized using SHELL181 elements with Mindlin-Reissner formulation and a finite element mesh is constructed, which remains unchanged throughout the design process. The discretization of the domain should be fine enough to guarantee an accurate solution, a reasonably reduced computational cost and a clear resolution of the final topology. Material properties are defined for each element. Because the elastic moduli are iteratively updated during the optimization routines, an external text file is written, which univocally assigns to each finite element the corresponding fictitious elastic parameter. The use of an outer folder allows editing of only the updated variables, without affecting other operational commands. In this initial preparatory stage, unit elastic moduli are set for all finite elements, in order to store the solid element stiffness matrices ($\mathbf{K}_e^0$), related to the artificial densities through Eq. (10), and required for performing the sensitivity analyses. Loading and supporting conditions are also applied. In step (*iii*), the APDL script acquires the information needed to initialize the optimization algorithm, i.e. the coordinate data and the element stiffness matrices of the solid material. In detail, a nodal array stores the spatial position of each node (in the *x, y, z* coordinates) in the *node coordinate matrix* while an element array acquires information about the connectivity between elements and nodes. These data are indispensable for reproducing a univocal correlation of the element-node representation between Ansys and Matlab environments, i.e. the so-called *connectivity matrix*. The *solid element stiffness matrices* are then stored. Because the connectivity and the stiffness matrices are invariant during the optimization routines, it is possible to acquire this information only once at the beginning of the optimization run. To further speed up the optimization procedure, only information on the continuum domain is explicitly acquired in a text format, which can be directly converted and updated in the Matlab environment. Supplementary data on additional members of the mechanical model, which implicitly contribute to the global response, can be retrieved at any iteration, if necessary. A similar data structure is compact and easy to implement, as it employs only a small amount of memory usage while providing the user with information on the complete geometrical and mechanical model. This is particularly convenient in the case of large-scale models where the amount of records may require extensive storage space if not carefully considered, rendering their cost prohibitive.

Once the mechanical model is generated and the related data are stored, the topology optimization framework is initialized. The optimization routine starts with a preliminary homogeneous distribution of material within the domain. To this end, a vector of independent design variables $\mathbf{x}$ is firstly defined, which associates an artificial density value to each finite element of the domain. Furthermore, because topology optimization problems are generally prone to numerical instabilities, the framework applies a regularization technique [44], [49] to ensure existence of solutions and cope with checkboard patterns and mesh-dependent designs. The density filter performs a convolution product between a kernel and the design variable vector. As a result, the density of the element *e* is modified to be a function of the initial variable $x_e$ and of its neighboring elements, included within a region $N_e$ of fixed radius $r_{min}$, so that $\rho_e(x_{k\in N_e})$. The filtered densities $\rho_e$ are related to the mechanical properties of the element through the SIMP interpolation scheme of Eq. (6). At each step of the optimization procedure, the design variables are updated and the filtered densities $E_e(\rho_e)$ are iteratively overwritten in the external text file of the APDL script. Consequently, Ansys is called from Matlab to perform the finite element analysis of the complete structural model. The batch mode is especially beneficial in the case of optimization cycles, avoiding the need to directly operate on the finite element program. In addition, Ansys updates a database file (.db) at

each iteration, which provides the user with the possibility of monitoring the procedure in an iterative fashion. The file, indeed, contains the complete model generated during the finite element analysis. Therefore, it is always possible to retrieve information on stresses, strains, displacements and force reactions of all the members constituting the complete structure, at any time.

When the analysis terminates, the APDL script stores the resulting nodal displacements $\mathbf{u}(\boldsymbol{\rho})$. The displacement vector and the element stiffness matrices, in fact, are the only fields of interest required to solve the topology optimization problem.

After the objective function, the constraint function and the associated sensitivities with respect to the design variables are computed, the approach is well posed for solving the optimization problem in the form of Eq. (12). In order to update the design variables of the non-linear programming problem, the Method of Moving Asymptotes (MMA) [50] is adopted. The convergence of the problem, expressed in terms of changes between consecutive updates, is checked at each iteration. If the difference between two successive feasible solutions ($\left|x^{new} - x^{old}\right|$) is less than a convergence ratio $\varepsilon_i$, the optimization routine is stopped and the final layout printed. Otherwise, the optimization loop is repeated. The convergence ratio provides information on the stability of the optimality condition between the previous and the current iteration. It is commonly accepted that when the change of the compliance for two consecutive iterations is less than 10%, the optimization under the current volume constraint has reached a stable status [51]. When the convergence check is satisfied, the density matrix is converted into a grey-scale bitmap image, whereas each finite element can be translated into a pixel with discrete values of material densities, ranging between 0 and 1.

## 5 Numerical implementation

The integrated topology optimization framework described in the previous sections is employed here for defining the optimal layout of lateral resisting systems for tall buildings subject to wind loads. The optimal location of braces on the perimeter of tall buildings is generally determined by a trial and error procedure, which requires many iteration cycles and does not always guarantee the minimum amount of structural material to meet design requirements. Conversely, since the topology optimization framework is stated in terms of minimum compliance, which is a measure of the global stiffness within the structure, the optimal layout will always guarantee the attainment of the stiffest configuration to limit the lateral sway and the most economical arrangement for the structural components, at the same time. The focus of this section is to illustrate the applicability of shell elements within topology optimization procedures for three-dimensional tall building models and demonstrate the stability and efficiency of the proposed methodology in finding optimal solutions. For an efficient use of topology design, the problem is formulated on a test model (the ground structure) intentionally very simple to reduce the size of the analysis problem, thus the computational time of each iteration, and speed up the overall optimization routine without any loss of objectivity for the optimal solution. The reference model is a regular tall-building with a squared plan, as depicted in **Figure 4**.

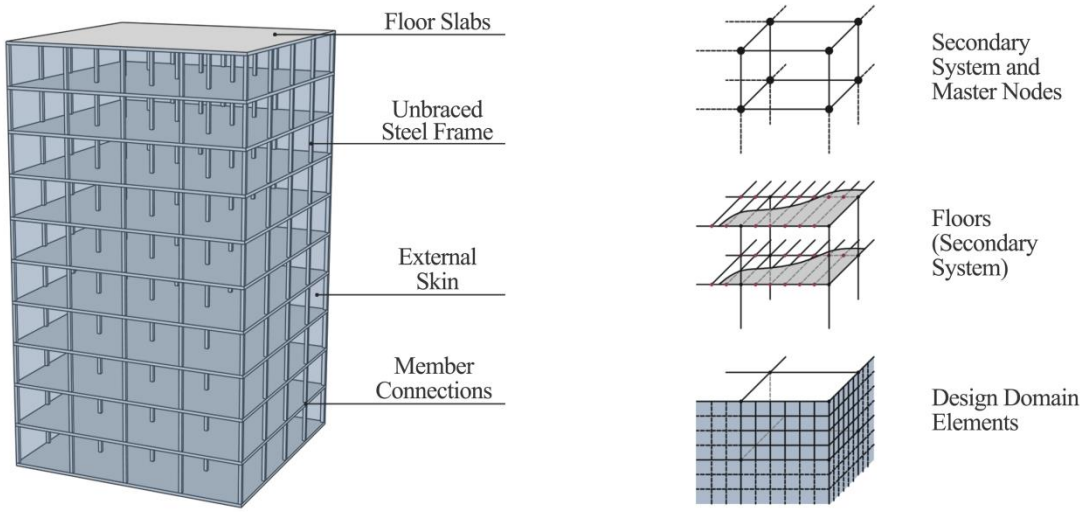


**Figure 4.** Model representation for the topology optimization procedure.

The external skin of the building is adopted as a natural optimizable domain $\Omega$. The geometric regularity of the building allows to impose two significant simplifications to the general problem: symmetry with respect to the centerline and doubly symmetric condition of the plan. Symmetry constraints are highly desirable in order to achieve a pattern repetition of the structural components of the tall building and minimize manufacturing costs [52], [53]. In addition, the introduction of a controlled regularization significantly reduces the amount of CPU-time, improves memory efficiency and allows the consideration of anti-symmetric loading scenarios.

The external loads acting on the building are reduced to two translational forces (acting in the longitudinal and transversal directions) for each floor, as depicted in **Figure 5**: the design domain located on the perimeter is subject to both in-plane and out-of-plane design forces. In fact, since wind can act in any horizontal direction, it is mandatory to determine and analyze both the forces along the building's longitudinal and transverse directions.

The optimal topology would certainly benefit from modeling a realistic loading scenario. However, in a preliminary design stage, a uniformly distributed load is generally considered to be sufficiently accurate and avoids adding further complexity to the problem.

Since the direct application of forces on the continuum designable domain could affect the objectivity of the final layout, an auxiliary frame (also referred to as secondary system) is introduced, as shown in **Figure 4**. A complete system is fully defined by combining the continuum domain with the discrete elements of the secondary system, as already proposed in [32], [34]. All external loads enter the complete system at master nodes located at the intersections of the secondary system (black nodes in **Figure 5**). Because of this and provided the assumption that the auxiliary perimeter framework is not included in the optimizable domain, the final topologies are independent of the definition of the master nodes [34]. This allows to arbitrarily choose the secondary system bounding the continuum domain. The members of the unbraced frame are preliminary sized for gravity loads only according to strength requirements. It is straightforward to demonstrate that when wind forces are applied, a demand for additional material results at the base of the domain from the topology optimization procedure. It follows that, once the optimal layout of the perimeter braced frame is achieved, columns should be re-sized for lateral loads before performing conclusive analyses on the optimized structural system. The elements constituting the auxiliary unbraced frame are discretized into smaller members, so that the nodes of the beam-column elements and those of the shell elements coincide. This operation results in a continuous connection between the discrete frame and the continuum domain, forcing the shell elements to move accordingly

with the deformation of the neighboring members, since they share three translational and three rotational degrees of freedom throughout the height and width of the building.

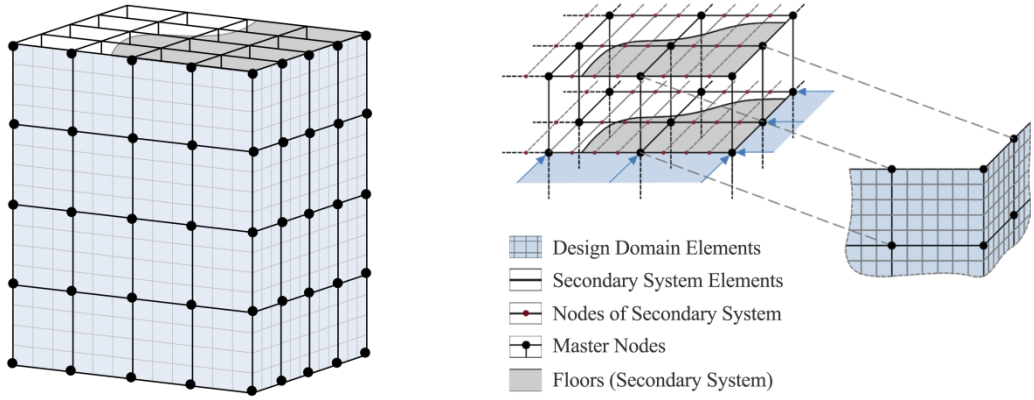


**Figure 5.** Schematic of the constitutive elements of the numerical model.

### 5.1 Case study

Numerical applications of the framework developed in this paper are presented in this section for the cases of a three-dimensional high-rise buildings. In order to investigate the efficiency of the proposed procedure in finding optimal solutions without the occurrence of numerical instabilities, a careful study on the mesh refinement is conducted. The 3D reference model has a height of 40 m and a plan of 12 m by 12 m, with a floor height of 4 m. On the perimeter, an outer lateral load resisting braced frame is designed by means of the proposed optimization framework. The structure is fully fixed at the base. The design dead load is assumed to be 7.0 kN/m$^2$. Live loads of 2.0 kN/m$^2$ are applied as uniformly distributed on the floor slabs.

An auxiliary perimeter framework bounding the continuum domain is arbitrarily chosen with a bay width of 3 meters and a bay height of 4 meters. W8x21 steel cross-sections are preliminary designed to model both the columns and the beams of the unbraced frame.

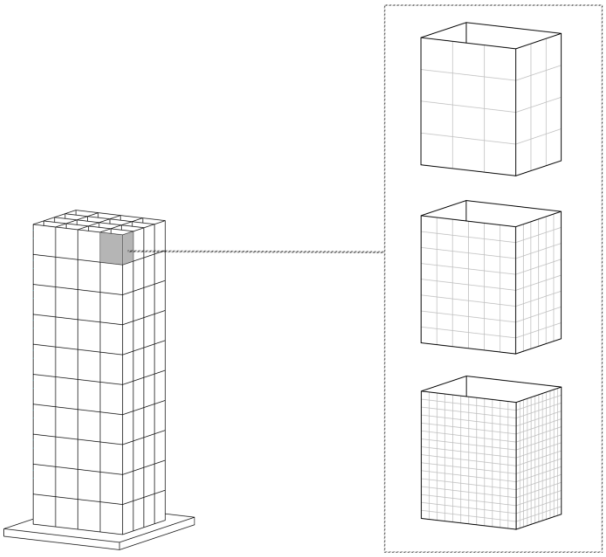

**Figure 6.** Design domain of the reference model (40 m x 12 m x 12 m) discretized using three mesh sizes: from the top 1 m x 1 m, 0.5 m x 0.5 m and 0.25 m x 0.25 m.

By the definition of this gravity system, external wind loads can be reduced to point loads, acting on the perimeter of each floor, and afterwards transferred to the lateral load resisting system [34]. The topology of the optimal braced frame is designed considering a lateral load with uniform distribution along the height of the building. Point forces of 100 kN are applied at each beam-to-column façades master node of the secondary system.

The topology optimization problem is stated in terms of minimum compliance with a constraint on the amount of volume available Eq. (12). The framework is performed according to the scheme depicted in **Figure 3**. The algorithm is run with a volume fraction of 30% and a projection radius of $r_{min}$=1.5 m. A penalization factor of $p$ = 3 is used, since it has been shown to provide good convergence properties to binary (0-1) solutions. The complete numerical model is analyzed using two types of finite elements, chosen from Ansys library. Three-dimensional two-node beams (BEAM188) with six degrees of freedom at each end and based on the Timoshenko beam theory are set for both the beams and columns. Four-node shell elements (SHELL188) with six degrees of freedom at each node are assigned to the floor slabs and the design domain. Floor slabs connecting the external faces of the building at each level are designed to be a C28/35 concrete deck (E=25 GPa) with a thickness of 0.10 m and a mesh size of 3x3 m. The continuum design domain is modeled using shell elements with Mindlin-Reissner formulation and the material properties of steel S275 (E=210 GPa) and a thickness of 0.15 m. The models are analyzed through static analysis in the elastic field. The design domain is optimized using three different mesh sizes as illustrated in **Figure 6**: 1 m x 1 m (resulting in 1,920 finite elements), 0.5 m x 0.5 m (7,680 elements) and 0.25 m x 0.25 m (30,720 elements). The utilization of homogeneous shells for the domain removes the necessity for the repeated computation of local stiffness matrices.

Although the mesh of the continuum design domain is refined, the loading conditions and the location of the secondary system do not change. This is an essential assumption in order to obtain comparable final topologies.

### 5.2 Results of the mesh refinement

Firstly, topology optimization is performed for the 40x12x12 m model with unit mesh size and the final topology is displayed in **Figure 7(a)** in terms of physical densities ($\boldsymbol{\rho}$), i.e. filtered design variables. As can be observed, the mesh is too coarse to achieve a feasible layout, since the size of finite elements is excessively large if compared to the model dimensions. Although a more detailed topology is needed to correctly define the working points between the diagonals and the column-to-brace connections, this initial result provides a preliminary evaluation of the material distribution within the domain. Furthermore, this initial step is indispensable in order to calibrate the optimization parameters of the subsequent stages and obtain qualitatively equivalent topologies. **Figure 7(b)** and **Figure 7(c)** show the optimal topologies obtained when refining the design domain using a mesh of 0.5 x 0.5 m and 0.25 x 0.25 m, respectively.

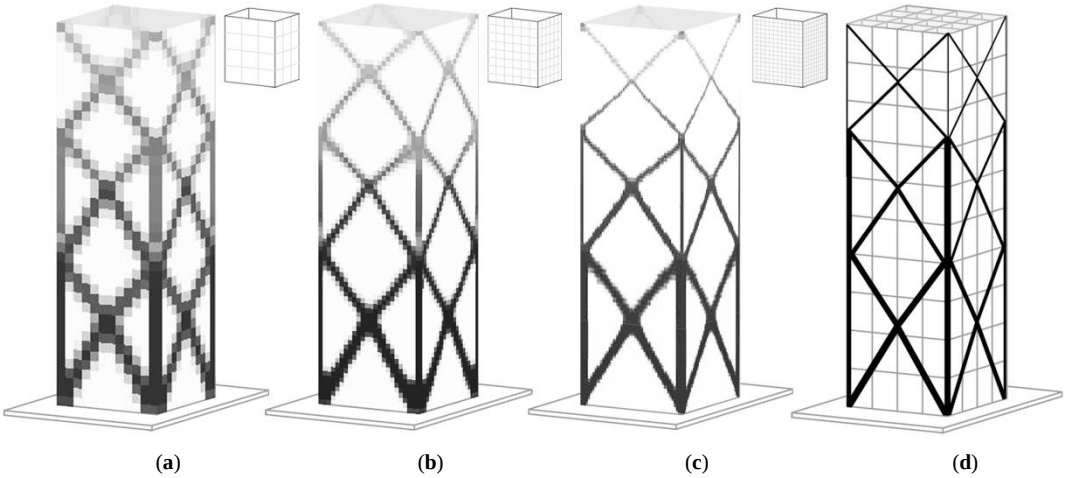

(**a**) (**b**) (**c**) (**d**)

**Figure 7.** Optimal topologies using mesh size of 1 m x 1m (**a**), 0.5 m x 0.5 m (**b**) and 0.25 m x 0.25 m (**c**) and post-processed refined layout (**c**).

The results clearly demonstrate that the optimal topologies remain qualitatively the same, despite significant differences of the boundaries of the domain, which become gradually smoother with mesh refinement. In fact, using a progressively finer mesh leads to increasingly improved resolution of the bitmap image and a more detailed definition of the members and the working points. In order to physically appreciate the results of the topology optimization process and correctly identify the location of the working points of the brace-to-brace and brace-to-column nodes, the optimized continuum domain is post-processed. In detail, all the pixels are subject to an image repair process to obtain the refined layout in **Figure 7(d)**. The topology optimization problem is stated in such a way that each structural member composing the optimal layout contributes to the global lateral stiffness by exhibiting a specific design which maximizes the overall stiffness while minimizing the total amount of structural material.

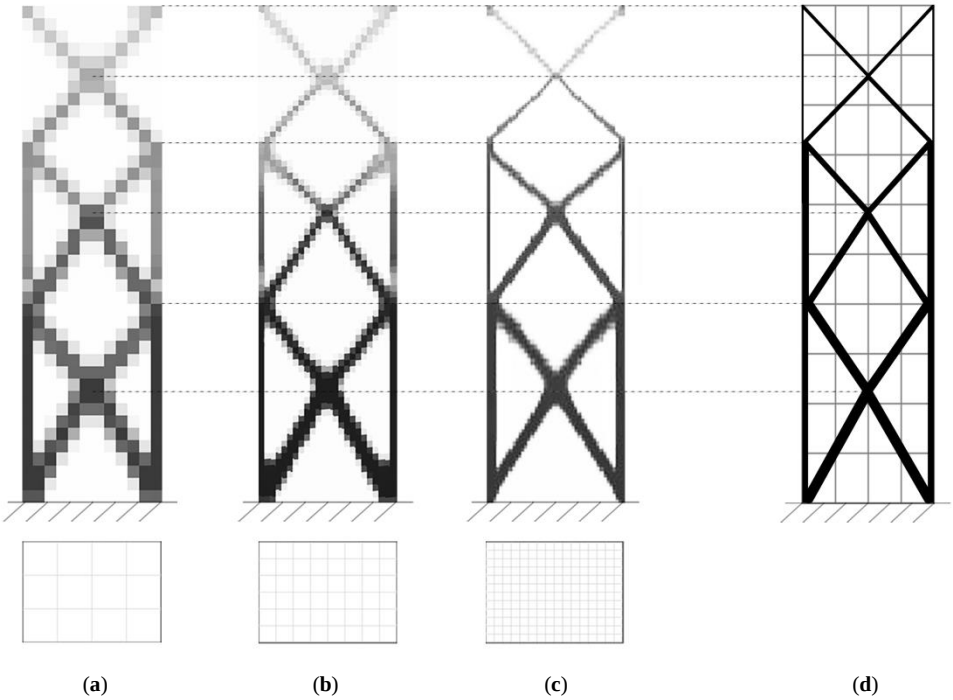

(**a**) (**b**) (**c**) (**d**)

**Figure 8.** Front views of optimal topologies: model with different mesh sizes: (**a**) 1x1 m, (**b**) 0.5x0.5 m and (**c**) 0.25x0.25 m; post-processed refined layout (**d**).

From the final layouts, three full width X-diagonals emerge, extending over a gradually reduced number of floors, from the bottom towards the top of the building, and with working points located at approximately mid-height of each module. Front views in **Figure 8** better show that vertical members should be sized to gradually increase their cross section along the height, in order to exhibit adequate flexural stiffness in accordance with the bending moment distribution of the vertical cantilever beam. However, it can be observed that the lateral columns on the top are interrupted before reaching the last module. This is caused by a very low value of intermediate densities and, of course, it is an unfeasible result. Because corner columns cannot be removed from the final braced system, they are introduced as very thin members in the discrete final layout (**Figure 8(d)**). Furthermore, it is worth noticing here that the optimal topology does not include the presence of the secondary system and, therefore, it can be omitted from the final layout. Such observation is consistent with the assumption on the arbitrary selection of the secondary system. Since symmetry constraints are enforced along the three axes, the topology optimization framework leads to identical layouts on each façade, such regularity is effective in simplifying the model through the replication of structural components.

The evolution of the optimal solution during the optimization routines can be appreciated in Figure 9 by considering the iteration histories of the objective function (mean compliance) and the constraint function (material volume) with respect to the number of iterations required until a tolerance of 1% is met. In the diagrams, the convergence to the optimal solution is emphasized using a filled circle at the end of the curves.

The validity and efficiency of the methodology is confirmed by the steady convergence as well as the limited number of optimization cycles required for all the three mesh-refining models. In order to evaluate the rapidity of the proposed framework in finding optimal solutions, additional information about the time consumption until convergence is provided in **Table 1**. It is worth clarifying here that almost 50% of the computation time is spent by Matlab to plot the intermediate optimized layouts, which can be conveniently eliminated from the main framework if not needed. Furthermore, the first iteration is generally slower (almost 35%) than the next ones due to the need to acquire mechanical and geometrical information of the model. However, for the sake of completeness, the computation time is calculated as the average over the first five iterations of the complete optimization routine, using a laptop with an Intel core i7-3610-QM, 2.30 GHz CPU, 4.00 GB memory. Refining a shell mesh to half of the element size requires approximately 2 times the number of iterations and 2.6 times the mean time per iteration with respect to a unit mesh size. Refining the mesh size to a quarter of the initial size requires more than 4.5 times the number of iterations and approximately 10 times the mean time per iteration with respect to the initial mesh size. The total time required to perform the overall optimization procedure for the mesh size of 0.5 m x 0.5 m and 0.25 m x 0.25 m is 5.5 times and more than 45 times the unit mesh size, respectively.

**Table 1.** Comparison of the time consumption between the analyzed models.

| **Mesh size** ($m^2$) | **No. of Iterations** (-) | **Mean time per iteration** (sec) | **Total required time** (h) |
|---|---|---|---|
| 1x1 | 173 | 6.00 | 0.28 |
| 0.5x0.5 | 352 | 16.00 | 1.55 |
| 0.25x0.25 | 782 | 59.00 | 12.80 |

(a)

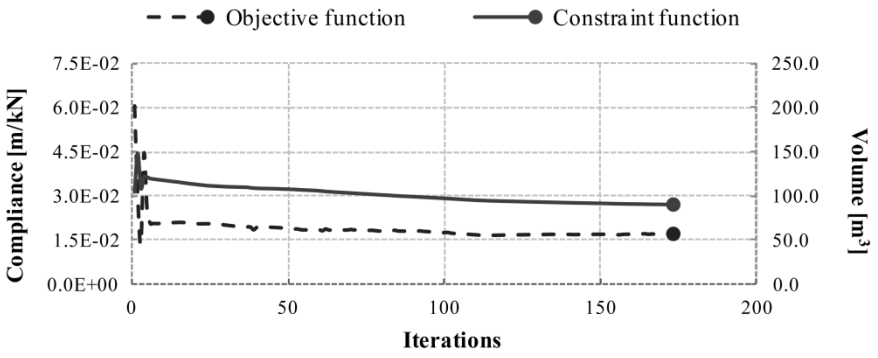


(b)

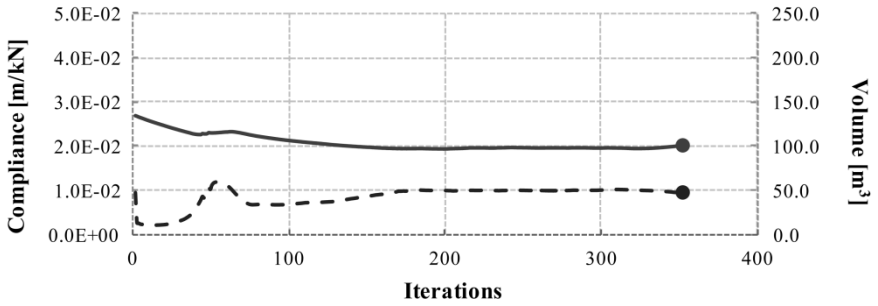


(c)

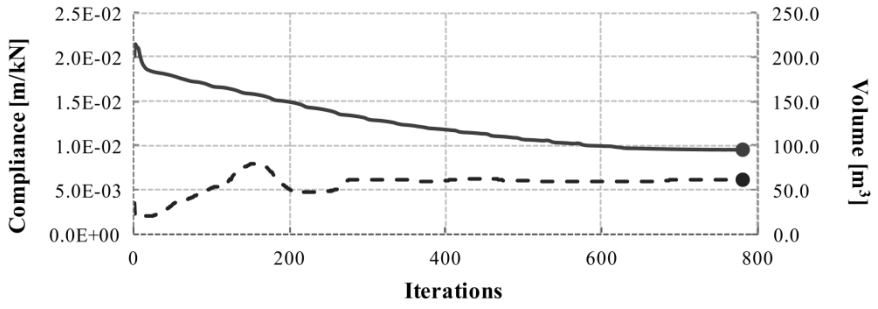


**Figure 9**. Iteration histories of the objective and constraint functions for the model with different mesh sizes: (a) 1x1 m, (b) 0.5x0.5 m and (c) 0.25x0.25 m.

In order to estimate the actual contribution of loads acting on the mid-surface of the shell elements as well as transverse loads, the in-plane and out-of-plane components of the wind action on the continuum domain are separately considered in **Figure 10**. The stress distributions of the Mindlin-Reissner shells, extracted from Ansys, are expressed in kN/m$^2$ and refer to a representative façade of the optimized model with mesh size of 1 m x 1 m. Because of the adoption of symmetry constraints and the proven mesh independent solutions, similar results occur for the other faces and other mesh refinements, respectively. It is worth mentioning here that the incomplete stress distribution, especially in the upper part of the building model, is mainly due to low artificial density values. This, in turn, suggests a reduced use of structural material for the braces located at the top. Furthermore, the element solutions confirm that the optimal topology is characterized by a gradual increase in the stress/strain distribution towards the base, as a result of a gradual compliance (or stiffness) distribution along the elevation. Such features improve the overall mechanical performance of the structural system by preventing the occurrence of stress peaks, especially in the column-to-brace nodes and in the working points between the diagonals.

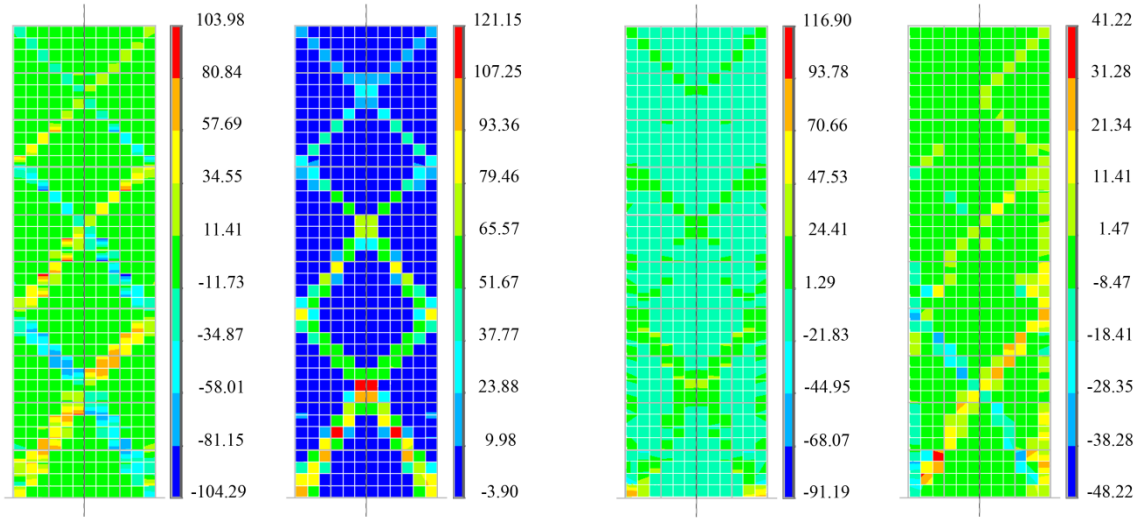


**Figure 10.** Stress and shear stress distributions for the pure in-plane component ((a) and (b), respectively) and pure out-of-plane component ((c) and (d), respectively) of the wind loading.

### 5.3 Comparison between 2D and 3D results

This section outlines the difference between optimal solutions obtained using a 2D planar model, envisioned as part of the 3D building, with those obtained by considering the complete structure. The same reference model (40 meters height and 12 meters width) is considered here. It is worth noticing that because two-dimensional models are loaded in their mid-plane, actually the shell behavior is reduced to that of a membrane with only in-plane stiffness. The iterative history and the resulting layout of the planar design domain are shown in **Figure 11**.

The mean elapsed time until convergence for the 2D model using a mesh size of 1m x 1m is around 3.5 seconds per iteration. The same observation made above for 3D domains concerning the elapsed to plot intermediate optimal layouts is also valid here. Comparing the 2D and 3D post-processed layouts in **Figure 12**, it emerges that the optimal results are quite similar when a model with a low aspect ratio is assumed as in the case under examination (aspect ratio equal to 3.3). However, some peculiarities emerge focusing on the diagonal arrangement and the working point locations. In fact, the optimization process leads to a gradually varying inclination for braces along the height of the building in the two-dimensional domain [54]. According to the literature, the optimal location of the working points lies in a feasible region delimited by a lower bound of 0.50 $h$ and an upper bound of 0.75 $h$, where $h$ is the module height [55]. This leads to a brace-to-brace angle of around 45 degrees at the top and X-high waisted diagonals near the base. As a consequence, a progressive translation of between these two values can be observed along the height of the building in **Figure 12(a)**. Conversely, in three-dimensional cases, the final topology is strictly related to the number of stories within each module and their location with respect to the optimizable domain (i.e. the inter-story height), both of which are information usually defined in advance in the design of tall buildings. Therefore, 3D systems are more sensitive to loading and modeling variations, producing the stretching effect of the diagonals over a largest number of floors in **Figure 12(c)**. The introduction of a complete 3D floor system moves the optimal layout away from the theoretical 2D optimal configuration, as it not only results in an increase of the gravity load but the vertical action of floors also insists along the diagonal length. Since the bracing member expands over a certain number of stories, in fact, the transfer of loads occurs at each floor level, producing concentrated loads along the diagonal length. Bending moments and shear forces arise due to this state. Furthermore, a deeper evaluation of the optimal topology can be assessed by observing the stress trajectory distribution of a cantilever beam with hollow tube section in **Figure 13**.

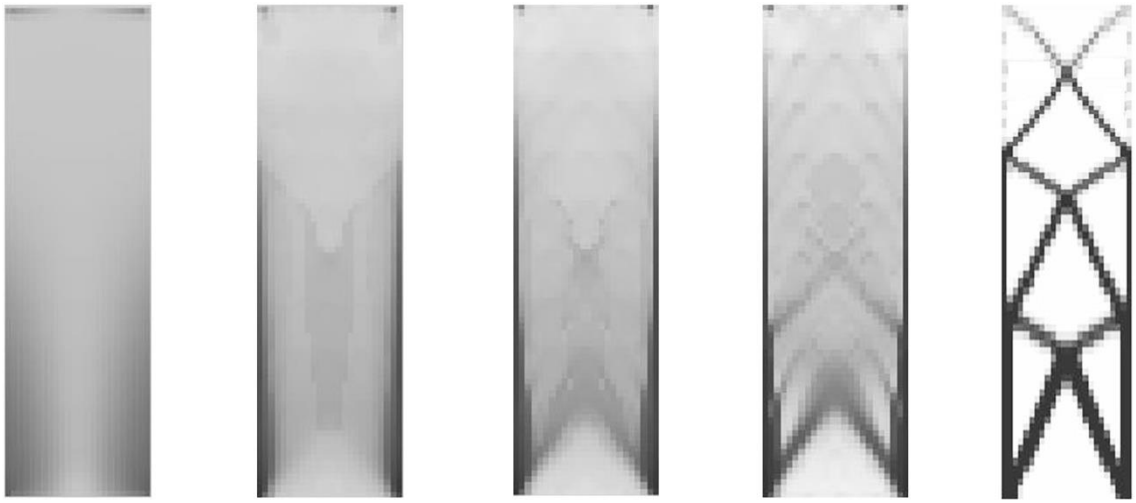

**Figure 11.** Iterative history and final optimal topology for the 2D model.

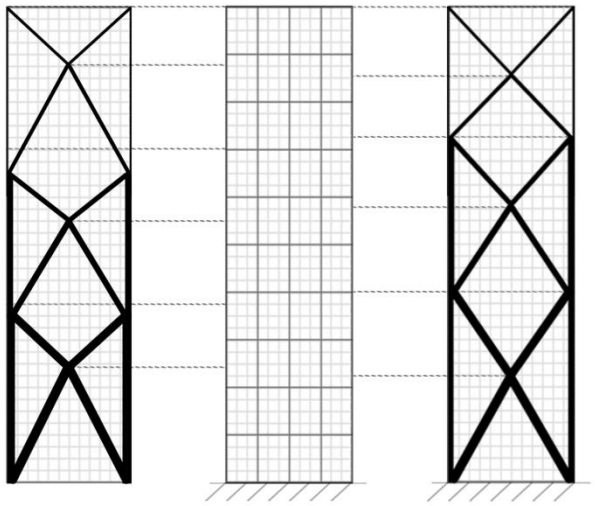

(**a**) (**b**) (**c**)

**Figure 12.** 2D optimal results, design domain and front view of the 3D optimal layout for the 40 x 12 x 12 m model (**a**, **b**, **c** respectively) using a mesh size of 0.5 x 0.5 m.

The principal stress directions are a good indicator of the optimization tool efficiency, since they inform on the natural flow of forces throughout the structure, i.e. where adding or removing structural material is favorable. The stress trajectories in the web panel, parallel to wind direction, behave similarly to the two-dimensional problem analyzed in **Figure 11**. On the other hand, the flange panel orthogonal to wind direction presents vertical stress trajectories [56]. The different behavior of the building façades allows considering two flange sides mainly carrying the overturning moment and two web sides carrying the shear force. When the external loads acting on the building are reduced to two translational forces, in order to simulate the aleatory action of wind, an intermediate condition arises on each panel. The vertical component of the overturning moment (due to the out-of-plane forces) together with the gravity action of the floor slabs produces higher flexural demands for the diagonal members.

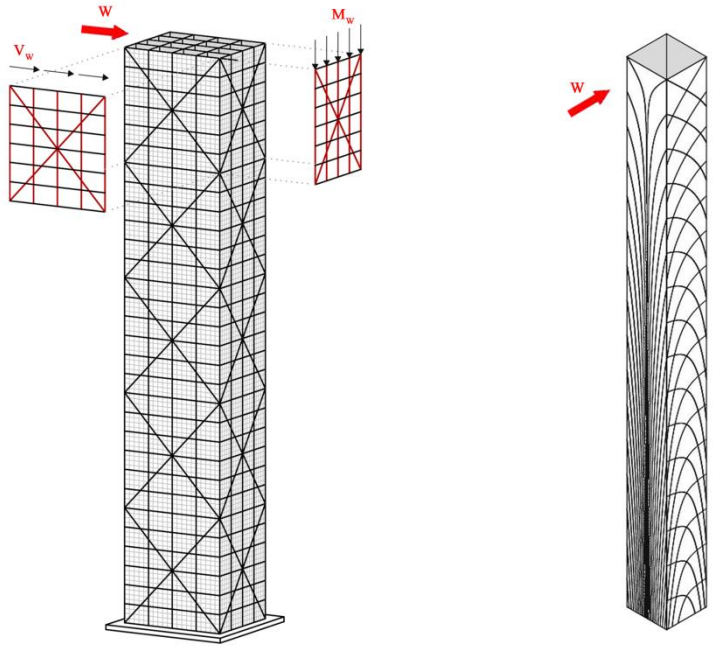


(**a**) (**b**)

**Figure 13.** Schematic of the mechanical behavior of braced tube systems (**a**) and stress trajectories of a cantilever beam [56] (**b**).

This results in a progressively steeper configuration against more severe loading conditions, observable in the vertical translation of the working points, which are lowered towards mid-height of the module when compared to the 2D layout. According to these considerations and since the final topologies resulting from the 2D and 3D models are qualitatively different, it is clear that a spatial model is highly desirable in order to achieve more reliable and objective optimal layouts. A three-dimensional design domain, in fact, reduces the amount of modeling and loading simplifications, allowing to consider more realistic scenarios for the topology optimization problem.

## 6 Conclusions

The paper presents an integrated framework for topology optimization of three-dimensional buildings using shell elements for the discretization of the design domain. The proposed methodology is envisioned for the preliminary design phase of structural systems for tall buildings, demonstrating the potentials of automated techniques in exploring innovative and efficient design solutions for large-scale domains. In particular, the framework incorporates a complete and efficient optimization algorithm with the advanced capabilities of Ansys for the assessment of optimal layouts for three-dimensional geometries, generated in CAD environments. The paper proposes the adoption of shell elements within topology optimization procedures to discretize the designable domain of three-dimensional tall buildings. In fact, given the potential of shells in describing loads acting on the mid-surface of the element, as well as transverse loads, these elements are especially convenient for simulating tubular high-rise buildings with perimeter structural system under wind actions.

This procedure offers the possibility to explore optimal layouts for standard or unconventional three-dimensional designs. The applicability and potential of the approach are validated by performing the topology optimization of a three-dimensional tall building. A case study with gradually refined mesh sizes is presented in order to demonstrate the efficiency of the proposed framework in finding optimal solutions free from numerical mesh-dependency instabilities. A further study is conducted by comparing the optimized resisting system of the reference tall building when planar and three-dimensional domains are

adopted. The main differences between the two modeling approaches emerge when focus is placed on the arrangements of the diagonal members. For two-dimensional domains, the optimization process leads to a gradually varying inclination for braces along the height of the building. Conversely, three-dimensional domains are seen to be more sensitive to loading and modeling variations, resulting in diagonals that stretch over a larger number of floors. In fact, for three-dimensional domains, the final topology is strictly related to the number and location of the stories as well as to the transverse action of the out-of-plane component of the wind load. The introduction of a complete three-dimensional model of the floor system together with a comprehensive modeling of the loading scenario moves the optimal layout away from the theoretical two-dimensional optimal configuration. Such a modeling approach is made possible by the adoption of shell elements for the discretization of the continuum domain of the building.

This paper demonstrated that the implementation of shell elements within topology optimization frameworks allows the assessment of accurate and reliable solutions, given the possibility of assuming realistic modeling and loading conditions. The use of shells within the proposed integrated framework shows good stability and predictability properties together with a rapid convergence rate, which makes it especially suitable for the analysis of three-dimensional large-scale engineering problems, as in the case of tall buildings. While the adoption of shell elements within two-dimensional topology optimization procedures naturally involves a greater number of degrees of freedom (which in turn produces higher computational costs) than membrane elements, they represent a convincing option for the discretization of three-dimensional domains. In fact, shells require fewer elements compared to solid bricks, which are often implemented in performing three-dimensional topology optimizations. This significantly reduces the number of equations to be solved during finite element analyses and makes the use of shell elements more convenient than solid elements for iterative algorithms. Additionally, since shells can model curved and free-form designs, they are especially suitable for the discretization of complex geometries and represent a valid alternative for performing topology optimization of modern designs.

## Acknowledgments

This work was partially supported by the Italian Ministry of Instruction, University and Research (MIUR). This support is gratefully acknowledged. Any opinions, findings, and conclusions or recommendations expressed in this paper are those of the authors and do not necessarily reflect those of the sponsor. The authors thank Krister Svanberg for providing the MMA algorithm, which was used as the optimization algorithm in this research.

## References

[1] M. P. Bendsøe and N. Kikuchi, “Generating optimal topologies in structural design using a homogenization method,” *Computer Methods in Applied Mechanics and Engineering*, vol. 71, no. 2, pp. 197–224, 1988.

[2] M. P. Bendsøe, “Optimal shape design as a material distribution problem,” *Structural Optimization*, vol. 1, no. 4, pp. 193–202, 1989.

[3] Z. Liu, J. G. Korvink, and R. Huang, “Structure topology optimization: fully coupled level set method via FEMLAB,” *Structural and Multidisciplinary Optimization*, vol. 29, no. 6, pp. 407–417, 2005.

[4] W. Hunter, “Predominantly solid-void three-dimensional topology optimisation using open source software.,” University of Stellenbosch, PhD Thesis, 2009.

[5] T. Sokół, “A 99 line code for discretized Michell truss optimization written in Mathematica,” *Structural and Multidisciplinary Optimization*, vol. 43, no. 2, pp. 181–190, 2011.

[6] O. Sigmund, “A 99 line topology optimization code written in Matlab,” *Structural and multidisciplinary optimization*, vol. 21, no. 2, pp. 120–127, 2001.

[7] E. Andreassen, A. Clausen, M. Schevenels, B. S. Lazarov, and O. Sigmund, “Efficient topology optimization in MATLAB using 88 lines of code,” vol. 43, no. 1, pp. 1–16, 2011.

[8] M. Y. Wang, X. Wang, and D. Guo, “A level set method for structural topology optimization,” *Computer methods in*

*applied mechanics and engineering*, vol. 192, no. 1–2, pp. 227–246, 2003.

[9] V. J. Challis, "A discrete level-set topology optimization code written in Matlab," *Structural and multidisciplinary optimization*, vol. 41, no. 3, pp. 453–464, 2010.

[10] N. Aage, M. Nobel-Jørgensen, C. S. Andreasen, and O. Sigmund, "Interactive topology optimization on hand-held devices," *Structural and Multidisciplinary Optimization*, vol. 47, no. 1, pp. 1–6, 2013.

[11] C. Talischi, G. H. Paulino, and C. H. Le, "Topology optimization using Wachspress-type interpolation with hexagonal elements," in *AIP Conference Proceedings*, 2008, vol. 973, pp. 309–314.

[12] L. L. Beghini *et al.*, "Integrated Discrete / Continuum Topology Optimization Framework for Stiffness or Global Stability of High-Rise Buildings," vol. 04014207, no. 10, pp. 1–10, 2015.

[13] C. Talischi, G. H. Paulino, A. Pereira, and I. F. M. Menezes, "PolyMesher: A general-purpose mesh generator for polygonal elements written in Matlab," *Structural and Multidisciplinary Optimization*, vol. 45, no. 3, pp. 309–328, 2012.

[14] C. Talischi, G. H. Paulino, A. Pereira, and I. F. M. Menezes, "PolyTop : a Matlab implementation of a general topology optimization framework using unstructured polygonal finite element meshes," pp. 329–357, 2012.

[15] A. Pereira, I. F. M. Menezes, C. Talischi, and G. H. Paulino, "PolyTop3D: a three-dimensional Matlab implementation of topology optimization using unstructured polyhedral finite element meshes," in *Blucher Material Science Proceedings*, 2014, p. 87.

[16] E. Aranda, J. C. Bellido, and A. Donoso, "Toptimiz3D: A topology optimization software using unstructured meshes," *Advances in Engineering Software*, vol. 148, no. December 2019, p. 102875, 2020.

[17] K. Liu and A. Tovar, "An efficient 3D topology optimization code written in Matlab," *Structural and Multidisciplinary Optimization*, vol. 50, no. 6, pp. 1175–1196, 2014.

[18] O. Amir and O. Sigmund, "On reducing computational effort in topology optimization: How far can we go?," *Structural and Multidisciplinary Optimization*, vol. 44, no. 1, pp. 25–29, 2011.

[19] F. Ferrari and O. Sigmund, "A new generation 99 line Matlab code for compliance Topology Optimization and its extension to 3D," 2020.

[20] Z. H. Zuo and Y. M. Xie, "A simple and compact Python code for complex 3D topology optimization," *Advances in Engineering Software*, vol. 85, no. MARCH, pp. 1–11, 2015.

[21] A. Shariati, R. Kamgar, R. Rahgozar, C. Science, and T. Park, "Optimum layout of nonlinear fluid viscous damper for improvement the responses of tall buildings," vol. 10, no. May, pp. 411–431, 2020.

[22] R. Kamgar, S. Shojaee, and R. Rahgozar, "Rehabilitation of tall buildings by active control system subjected to critical seismic excitation," vol. 16, no. 6, pp. 819–833, 2015.

[23] M. Dadkhah, R. Kamgar, H. Heidarzadeh, and A. Jakubczyk-gałczy, "Improvement of Performance Level of Steel Moment-Resisting Frames Using Tuned Mass Damper System," pp. 34–38, 2020.

[24] R. Kamgar, F. Gholami, H. Reza, Z. Sanayei, and H. Heidarzadeh, "Modified Tuned Liquid Dampers for Seismic Protection of Buildings Considering Soil – Structure Interaction Effects," *Iranian Journal of Science and Technology, Transactions of Civil Engineering*, vol. 44, no. 1, pp. 339–354, 2020.

[25] R. Kamgar, "Optimizing parameters of tuned mass damper subjected to critical earthquake," no. November 2017, pp. 1–16, 2018.

[26] M. Khatibinia, H. Gholami, and R. Kamgar, "Optimal design of tuned mass dampers subjected to continuous stationary critical excitation," *International Journal of Dynamics and Control*, vol. 6, no. 3, pp. 1094–1104, 2018.

[27] R. Tavakoli, R. Kamgar, and R. Rahgozar, "Optimal Location of Energy Dissipation Outrigger in High-rise Building Considering Nonlinear Soil-structure Interaction Effects," pp. 1–17, 2020.

[28] R. Kamgar and R. Rahgozar, "Determination of Optimum Location for Flexible Outrigger Systems in Tall Buildings with Constant Cross Section Consisting of Framed Tube , Shear Core , Belt Truss and Outrigger System Using Energy Method," vol. 17, no. 1, pp. 1–8, 2017.

[29] R. Tavakoli, R. Kamgar, and R. Rahgozar, "Seismic performance of outrigger – belt truss system considering soil – structure interaction," *International Journal of Advanced Structural Engineering*, vol. 11, no. 1, pp. 45–54, 2019.

[30] R. Kamgar and P. Rahgozar, "Reducing static roof displacement and axial forces of columns in tall buildings based on obtaining the best locations for multi - rigid belt truss outrigger systems," *Asian Journal of Civil Engineering*, vol. 20, no. 6, pp. 759–768, 2019.

[31] S. M. J. Spence and M. Gioffrè, "Large scale reliability-based design optimization of wind excited tall buildings," *Probabilistic Engineering Mechanics*, vol. 28, no. August, pp. 206–215, 2014.

[32] S. M. J. Spence and A. Kareem, "Performance-based design and optimization of uncertain wind-excited dynamic building systems," *Engineering Structures*, vol. 78, pp. 133–144, 2014.

[33] A. Suksuwan and S. M. J. Spence, "Performance-based multi-hazard topology optimization of wind and seismically excited structural systems," *Engineering Structures*, vol. 172, pp. 573–588, 2018.

[34] S. Bobby, S. M. J. Spence, and A. Kareem, "Data-driven performance-based topology optimization of uncertain wind-excited tall buildings," *Structural and Multidisciplinary Optimization*, pp. 1379–1402, 2016.

[35] G. Angelucci and F. Mollaioli, "Diagrid structural systems for tall buildings: Changing pattern configuration through topological assessments," *Structural Design of Tall and Special Buildings*, vol. 26, no. 18, p. e1396, 2017.

[36] K. Maute and E. Ramm, "Adaptive topology optimization of shell structures," *AIAA journal*, vol. 35, no. 11, pp. 1767–1773, 1997.

[37] M. Victoria, O. M. Querin, C. Díaz, and P. Martí, "The effects of membrane thickness and asymmetry in the topology optimization of stiffeners for thin-shell structures," *Engineering Optimization*, vol. 0273, no. April 2017, 2014.

[38] B. Li, H. Liu, Z. Yang, and J. Zhang, "Stiffness design of plate/shell structures by evolutionary topology optimization," *Thin-Walled Structures*, vol. 141, no. April, pp. 232–250, 2019.

[39] W. Zhang *et al.*, "Stress-related topology optimization of shell structures using IGA/TSA-based Moving Morphable Void (MMV) approach," *Computer Methods in Applied Mechanics and Engineering*, vol. 366, p. 113036, 2020.

[40] K. U. Bletzinger, "A consistent frame for sensitivity filtering and the vertex assigned morphing of optimal shape," *Structural and Multidisciplinary Optimization*, vol. 49, no. 6, pp. 873–895, 2014.

[41] B. Hassani, S. M. Tavakkoli, and H. Ghasemnejad, "Simultaneous shape and topology optimization of shell structures," *Structural and Multidisciplinary Optimization*, vol. 48, no. 1, pp. 221–233, 2013.

[42] B. Boroomand and A. R. Barekatein, "On topology optimization of linear and nonlinear plate problems," *Structural and Multidisciplinary Optimization*, vol. 39, no. 1, pp. 17–27, 2009.

[43] Q. H. Pham and D. H. Phan, "Polygonal topology optimization for Reissner–Mindlin plates," *Engineering with Computers*, vol. 1, no. 14, 2020.

[44] B. Bourdin, "Filters in topology optimization," *International Journal for Numerical Methods in Engineering*, vol. 50, no. 9, pp. 2143–2158, 2001.

[45] "ANSYS® Academic Research Mechanical, Release 18.1, Help System, Coupled Field, Analysis Guide, ANSYS." .

[46] E. Reissner, "The effect of transverse shear deformation on the bending of elastic plates," *J. appl. Mech.*, pp. A69–A77, 1945.

[47] K.-J. Bathe and E. N. Dvorkin, "A Four-node Plate Bending Element Based on Mindlin/ Reissner Plate Theory and a Mixed Interpplation," *International Journal for Numerical Methods in Engineering*, vol. 21. pp. 367–383, 1985.

[48] O. Sigmund, "Morphology-based black and white filters for topology optimization," *Structural and Multidisciplinary Optimization*, vol. 33, no. 4–5, pp. 401–424, 2007.

[49] J. K. Guest, J. H. Prévost, and T. Belytschko, "Achieving minimum length scale in topology optimization using nodal design variables and projection functions," *International Journal for Numerical Methods in Engineering*, vol. 61, no. 2, pp. 238–254, 2004.

[50] K. Svanberg, "The method of moving asymptotes – a new method for structural optimization," *International journal for numerical methods in engineering*, vol. 24, no. 2, pp. 359–373, 1987.

[51] C. Lin and F. Hsu, "An adaptive volume constraint algorithm for topology optimization with a displacement-limit," *Advances in Engineering Software*, vol. 39, no. 12, pp. 973–994, 2008.

[52] Q. Liang, "Effects of continuum design domains on optimal bracing systems for multistory steel building frameworks," in *Proc 5th Australas Congr Appl Mech*, 2007, p. 794.

[53] L. L. Stromberg, A. Beghini, W. F. Baker, and G. H. Paulino, "Topology optimization for braced frames: Combining continuum and beam/column elements," *Engineering Structures*, vol. 37, pp. 106–124, 2012.

[54] G. Angelucci, F. Mollaioli, and O. Alshawa, "Evaluation of optimal lateral resisting systems for tall buildings subject to horizontal loads," *ScienceDirect*, vol. 00, pp. 1–8, 2019.

[55] W. F. Baker, "Energy-Based Design of Lateral Systems," *Structural Engineering International*, vol. 2, no. 2, pp. 99–102, 1992.

[56] L. L. Stromberg, A. Beghini, W. F. Baker, and G. H. Paulino, "Application of layout and topology optimization using pattern gradation for the conceptual design of buildings," *Struct Multidisc Optim*, vol. 43, pp. 165–180, 2011.

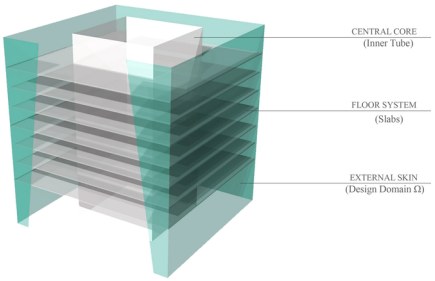


TAL_1817_Figure_1.tif

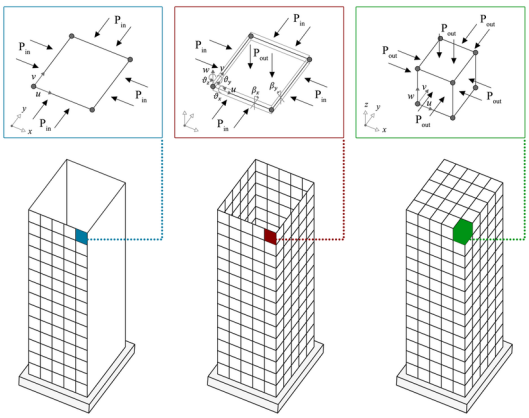

TAL_1817_Figure_2.tif

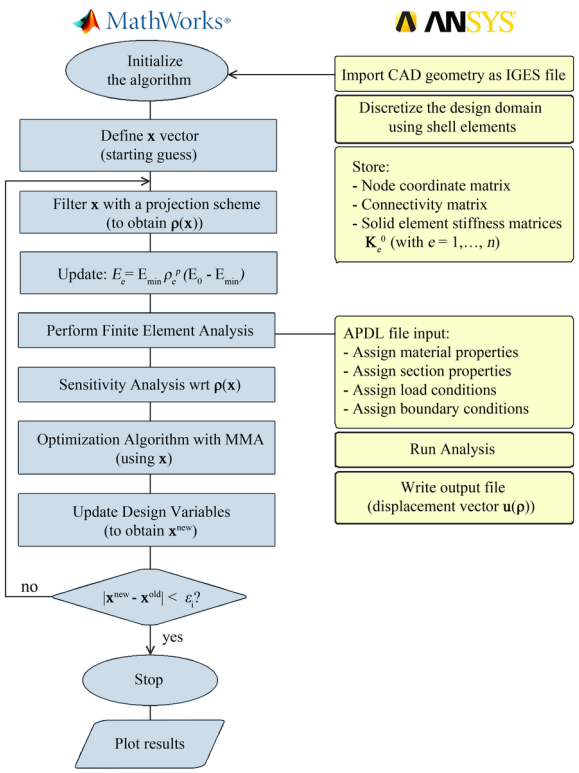


TAL_1817_Figure_3.tif

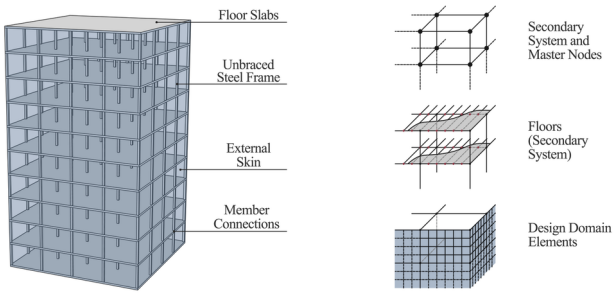


TAL_1817_Figure_4.tif

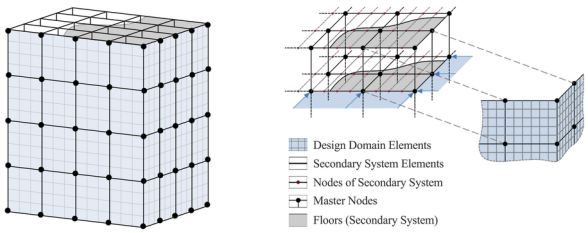


TAL_1817_Figure_5.tif

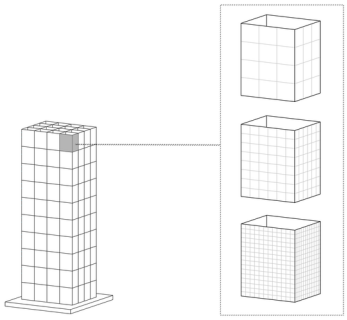

TAL_1817_Figure_6.tif

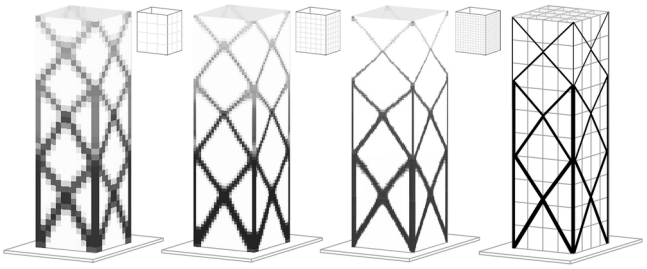

TAL_1817_Figure_7.tif

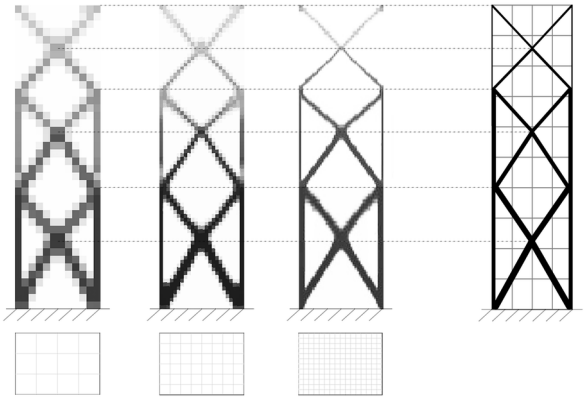

TAL_1817_Figure_8.tif

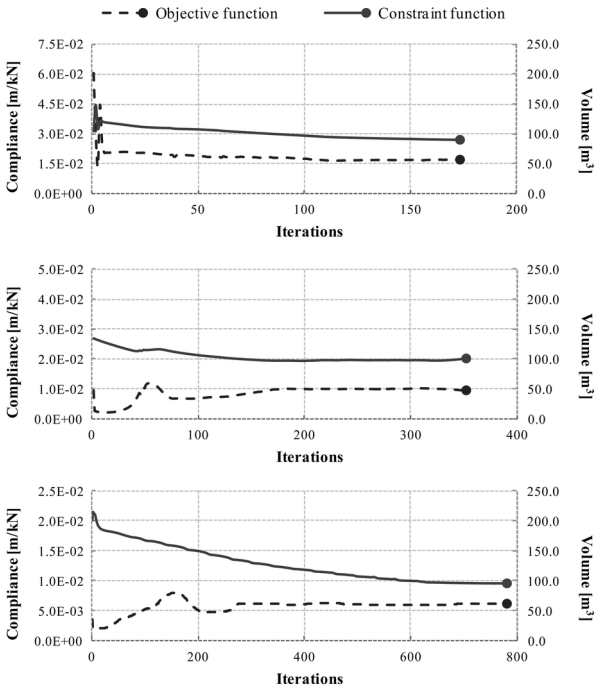


TAL_1817_Figure_9.tif

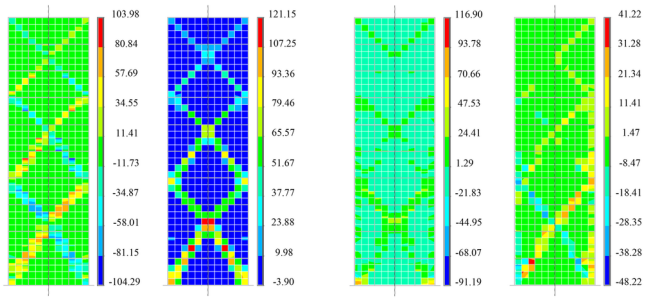


TAL_1817_Figure_10.tif

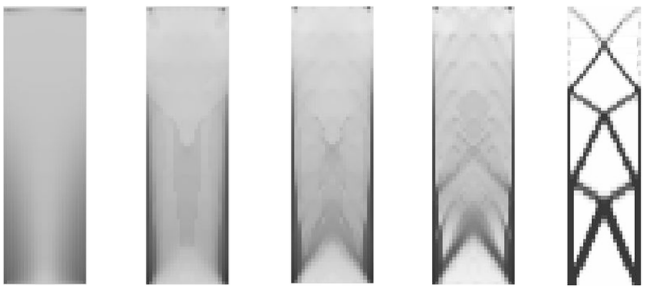

TAL_1817_Figure_11.tif

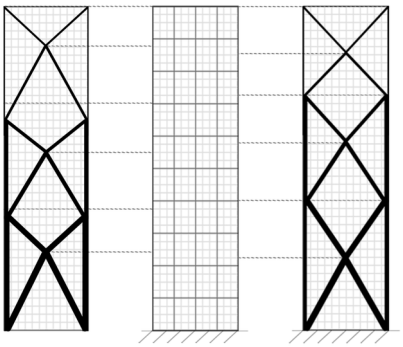

TAL_1817_Figure_12.tif

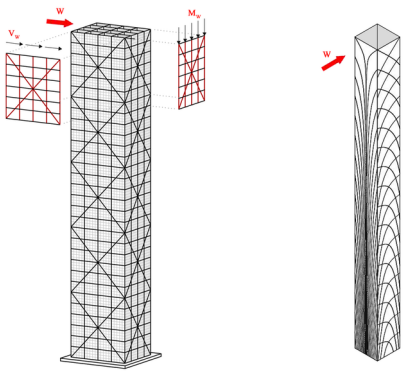


TAL_1817_Figure_13.tif